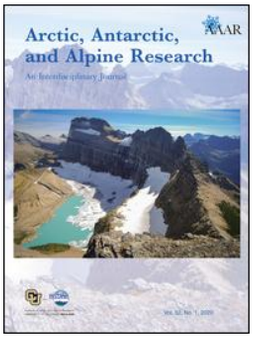

Arctic, Antarctic, and Alpine Research
An Interdisciplinary Journal

ISSN: 1523-0430 (Print) 1938-4246 (Online) Journal homepage: https://www.tandfonline.com/loi/uaar20

Water supply in times of climate change—Tracer tests to identify the catchment area of an Alpine karst spring, Tyrol, Austria

Rafael Schäffer, Ingo Sass & Claus-Dieter Heldmann

To cite this article: Rafael Schäffer, Ingo Sass & Claus-Dieter Heldmann (2020) Water supply in times of climate change—Tracer tests to identify the catchment area of an Alpine karst spring, Tyrol, Austria, Arctic, Antarctic, and Alpine Research, 52:1, 70-86, DOI: 10.1080/15230430.2020.1723853

To link to this article: https://doi.org/10.1080/15230430.2020.1723853

© 2020 The Author(s). Published with license by Taylor & Francis Group, LLC.

Published online: 11 Mar 2020.

Submit your article to this journal

Article views: 278

View related articles

View Crossmark data

Full Terms & Conditions of access and use can be found at
https://www.tandfonline.com/action/journalInformation?journalCode=uaar20

ARCTIC, ANTARCTIC, AND ALPINE RESEARCH
2020, VOL. 52, NO. 1, 70–86
https://doi.org/10.1080/15230430.2020.1723853

Taylor & Francis
Taylor & Francis Group

OPEN ACCESS Check for updates

Water supply in times of climate change—Tracer tests to identify the catchment area of an Alpine karst spring, Tyrol, Austria

Rafael Schäffer [a], Ingo Sass [a,b], and Claus-Dieter Heldmann [a]

[a]Institute of Applied Geosciences, Geothermal Science and Technology, Technische Universität Darmstadt, Darmstadt, Germany; [b]Darmstadt Graduate School of Excellence Energy Science and Engineering, Technische Universität Darmstadt, Darmstadt, Germany

ABSTRACT

Climate change and glacial retreat are changing the runoff behavior of Alpine springs and streams. For example, in the extremely dry and hot summer of 2018, many springs used for drinking water supply lost up to 50 percent of their average discharge; a few springs have even run dry. In order to ensure drinking water supply in the future, springs featuring large and constantly sufficient discharge rates will have to be identified and tapped. A case study was undertaken at the Tuxbachquelle because catchment area and temporal variation of physicochemical and hydrochemical properties were previously unknown. Tracer tests with uranine proved a hydraulic connection between this karst spring and a stream a few kilometers uphill. At low runoff, uranine needed about 4½ hours from the sink to the spring, whereas at high runoff more than four days was required. It became evident that discharge, electrical conductivity, temperature, and turbidity of the Tuxbachquelle respond within a few hours to precipitation events. The water quality and an examination of the water balance resulted in a significantly larger catchment area. It is assumed that widely karstified calcite marble subterraneously drains a considerable part of the Tuxertal (Tux Valley), including some active rock glaciers.

ARTICLE HISTORY
Received 20 June 2019
Revised 18 December 2019
Accepted 23 December 2019

KEYWORDS
Uranine; karst; discharge/runoff; rock glaciers; Hochstegen Formation

Introduction

Motivation

The importance of glaciers and rock glaciers as water reservoirs and for hydropower generation should be reevaluated for the future. Between 1850 and 2011, glaciers in the Zillertal Alps lost about two thirds of their area (Fischer et al. 2015). Within the Tuxertal (Tux Valley), the glacier area reduced from 20.6 km^2 to 7.1 km^2 between 1850 and 2004 (Pröbstl and Damm 2009). Based on the latest Tyrolean Geographic Information System (tiris) orthophotos of 2016 (Tyrolean Geographic Information System 2019), the glacier area totals only 5.2 km^2. The loss of glacial area and volume depends on several factors. Though no losses or slight glacier advances were observed in the 1970s and 1980s, there has since been a significantly accelerating glacier retreat (Gross 1987; Schwendiger and Pindur 2013; Fischer et al. 2015). Minor glaciers smaller than 2 km^2 are much more affected by the decline than larger glaciers (Schwendiger and Pindur 2013). Ice loss occurs mainly at altitudes lower than 3,200 m. a.s.l., where small glaciers are dominantly situated (Lambrecht and Kuhn 2007). With respect to the catchment areas of big Alpine rivers, such as the Rhône, Rhine, or Inn, the contribution of glacier melt reaches up to 25 percent of the total summer runoff (Huss 2011). Small catchment areas of several square kilometers can derive their runoff almost completely from meltwater. Permafrost and dead ice melt may add significant proportions and influence water composition (Winkler et al. 2016; Colombo et al. 2018; Brighenti et al. 2019).

Almost all active rock glaciers in eastern North Tyrol are located in the Tuxertal. The area of these active rock glaciers in the Tux Alps is estimated at 2.2 km^2. The surface of another 230 inactive or fossil rock glaciers amounts to 9.1 km^2 (Krainer and Ribis 2012). Active rock glaciers can feature daily varying influences on discharge rates, chemical compositions including heavy metal concentrations, and physical properties of downstream streams and springs (Krainer and Mostler 2002; Thies et al. 2013; Nickus, Thies, and Krainer 2015).

The Alps are more strongly affected by climate change than other regions (Auer et al. 2007; Brunetti

CONTACT Rafael Schäffer schaeffer@geo.tu-darmstadt.de Institute of Applied Geosciences, Geothermal Science and Technology, Technische Universität Darmstadt, Schnittspahnstrasse 9, Darmstadt 64287, Germany.

© 2020 The Author(s). Published with license by Taylor & Francis Group, LLC.
This is an Open Access article distributed under the terms of the Creative Commons Attribution License (http://creativecommons.org/licenses/by/4.0/), which permits unrestricted use, distribution, and reproduction in any medium, provided the original work is properly cited.

et al. 2009). It can be demonstrated that climate change has led to significant changes in precipitation and the runoff behavior of rivers during recent decades (Brunetti et al. 2006; Saidi et al. 2018). In addition, small catchment areas react immediately to weather extremes, such as the expected increase in heavy rainfall events or longer dry periods caused by climate change (Rajczak, Pall, and Schär 2013). It is therefore to be expected that springs at high elevations will be subject to larger discharge fluctuations and will dry out more frequently in the future. Climate models predict a time shift of the precipitation maxima from summer to winter as well as that precipitation will more often be in the form of rain instead of snowfall (Gobiet et al. 2014). The resulting change in runoff characteristics will be superposed by earlier snowmelt and a decrease in snow cover, especially below 2,000 m (Kobierska et al. 2013; Gobiet et al. 2014). Because the demand for electricity in winter is higher than that in summer, this effect is advantageous for hydropower production (Wagner et al. 2017). On the other hand, this is disadvantageous for the water supply, because in Austrian rural and tourist regions water consumption is increased by 40 to 120 percent during the summer period (BLFUW 2012).

The water supply in rural Austria is largely in private hands. Tributary valleys of the Zillertal are characterized by isolated single spring or single well water supplies. Typically, they have small catchment areas or hydraulic connections to fissures, fractures, and faults. To provide a reliable water supply, it is necessary to tap perennial springs with a sufficient long-term discharge rate. It is suspected that many small catchment areas will not fulfill this requirement due to ongoing climatic change. Although the Tuxbachquelle has been identified by water authorities as important for future water supplies, this spring has never been thoroughly investigated due to its inaccessibility. The exact number of outlets, discharge rates, and the catchment area were largely unknown. One tracer test was carried out at both low and high runoff. The results are not only relevant to the water supply but are also interesting for a tunnel currently under construction (Fliegl 2017), further geothermal exploration (Sass, Heldmann, and Lehr 2016; Sass, Heldmann, and Schäffer 2016), and nature conservation, because the area is located in the recently expanded area of the High Alps Nature Park Zillertaler Alps.

Study area

The study area is located on the northwestern edge of the Tauern Window, including several faults caused by nappe stacking. A more detailed description of the geological setting is given in Schäffer et al. (2018). The Tuxbachquelle (TQ) is situated within the 4-km-long and up to 60-m-deep gorge of the Tuxbach (Tux Creek) next to Finkenberg (Figure 1).

The Tuxbachquelle originates in the Jurassic Hochstegen Formation. The structural strike is about 60° ENE parallel to the valley and dips approximately 70° NNW. From base to top, the Hochstegen Formation contains thin layers of quartzite, phyllite, and brownish marble, followed by sequences of grayish-blue banded calcitic and dolomitic marbles. Within the footwall of the Hochstegen Formation, the topographically higher Ahorn Gneiss is exposed (Figure 1). It consists of orthogneisses, which are primarily augen gneiss. The contact between both units is described as autochthonous, parautochthonous, or allochthonous (Frisch 1968, 1980; Thiele 1976). Low mineralized, lime-unsaturated, and cold waters from the Ahorn Gneiss infiltrate the Hochstegen Formation, having a high karstification potential (Sass, Heldmann, and Schäffer 2016).

The Tuxertal is rich in caves like other regions of Austria built by calcareous rocks (Christian and Spötl 2010; Spötl, Plan, and Christian 2016). Almost forty caves are known in the middle and upper parts of the valley, and the ongoing glacier retreat has allowed new discoveries in recent years (Spötl 2009). There are two recently gauged and officially catalogued caves within the Tuxbach gorge. Goldbründl cave, located 35 m above the Tuxbach level, is at least 14 m long and 8 m deep and shows a very variable water level at its lower end of at least 20 m (Spötl and Schiffmann 2014). The mouth of the Goldbründl into the Tuxbach is located close to TQ-12 (Figure 2). Grabungshöhle is situated about 50 m further east, with a length of at least 31 m and a depth of 12 m (Spötl and Schiffmann 2014). In the lowest part of this cave, the noise of the flowing water is audible at times. Recent silt and clay deposits within the cave also indicate ongoing hydrological activity.

Preliminary investigations

Several inspections of the Tuxbach gorge were carried out within several years, mainly during winter months due to the lower runoff and better accessibility. In the section between the Grinbergbach (Grinberg Creek) inflow and the confluence into the Zemmbach (Figure 1), only two springs have been observed.

The Tuxbachquelle consists of several outlets over a length of 80 m on the southern bank of the Tuxbach (Figure 2), numbered upstream from TQ-0 to TQ-12. All outlets are located at the river level, with the exception of

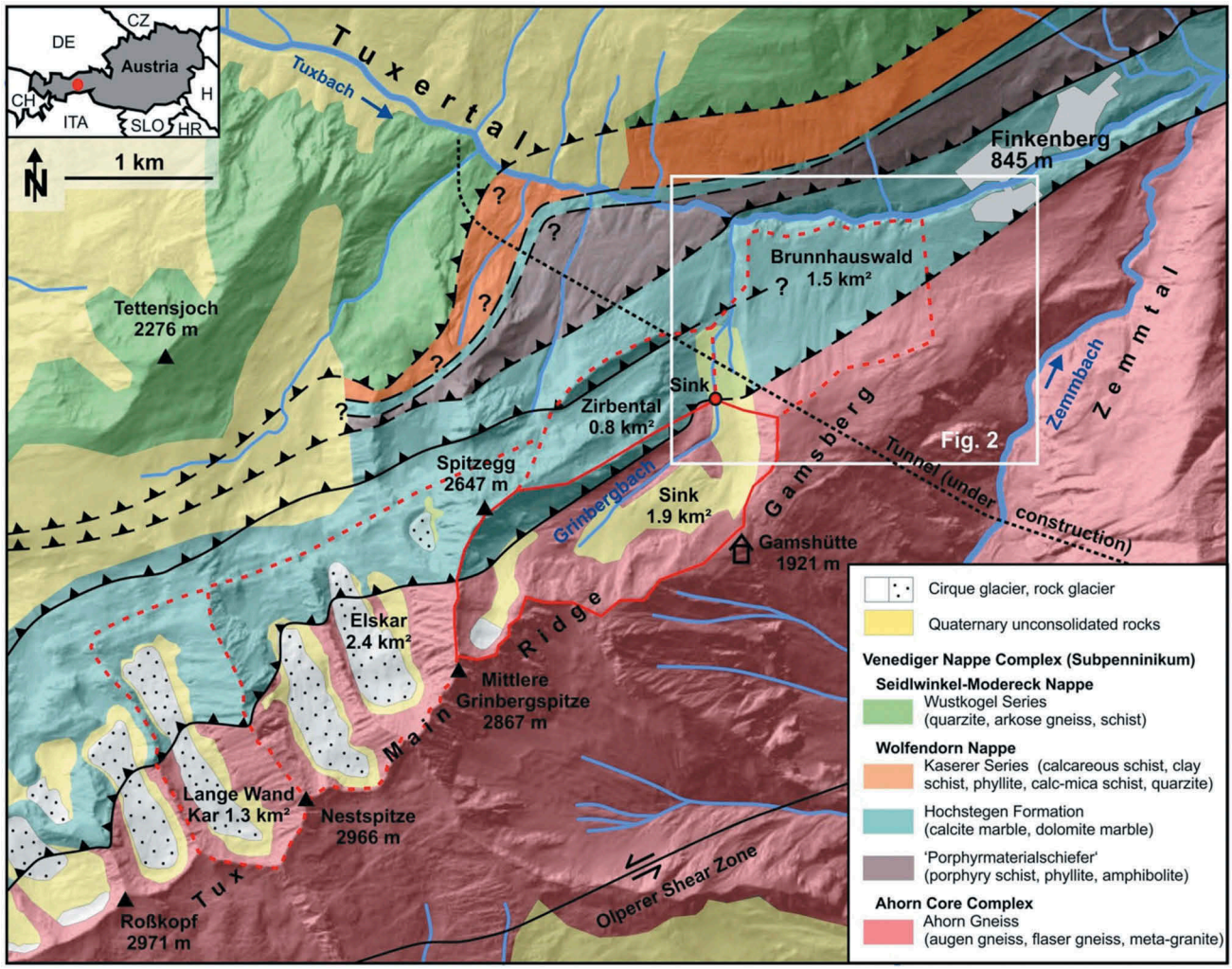

Figure 1. Simplified geological map of the project area, modified after Schäffer et al. (2018) and Kogler (2018). Relief shading was taken from the Tyrolean Geographic Information System (2019). The continuous red line indicates the catchment area of the sink; dashed red lines mark possible extensions of the catchment relating to the Tuxbachquelle.

TQ-6, which is located 3 m above the Tuxbach. Most outlets of the Tuxbachquelle are completely flooded during periods of high water and are hardly recognizable. Even at low water levels, the discharge of some outlets can only be estimated due to the short path into the Tuxbach and the low flow gradient. It became evident that TQ-1 is perennial. All other outlets are intermittent. The total discharge of the Tuxbachquelle varies from 70 to ca. 500 L/s. Goldbründl is intermittent and delivers up to ca. 500 L/s.

The Grinbergbach is the only perennial stream that drains the southern slope of the Tuxertal southwest of Finkenberg (Figure 1). In comparison to the Ahorn Gneiss, the density of water bodies is significantly lower in the Hochstegen Formation. Thus, it can be assumed that a considerable part of the drainage takes place underground.

A sink was identified in the riverbed of the Grinbergbach at 711 835 E, 5224 322 N at an altitude of 1,471 m (Figure 2). It likely was not recognized earlier for two reasons. First, the Grinbergbach only infiltrates completely at relatively low runoff rates. Secondly, quaternary deposits are filling this part of the hillside (Figure 1). There are various springs, featuring discharge rates of several liters per second each, emerging from unconsolidated rocks at a distance of 200 to 450 m below the sink (Figure 2). Thus, not only karstification but also expected high permeabilities of the quaternary deposits could explain the flow path of the Grinbergbach. However, comparisons of water temperature, electrical conductivity, and hydrochemical composition showed significant differences from the Grinbergbach above the sink. The western springs are conceivably fed by the Zirbental, which in karst morphology is defined as a dry valley. The catchment area of the eastern spring is probably the Gamsberg (Figure 2).

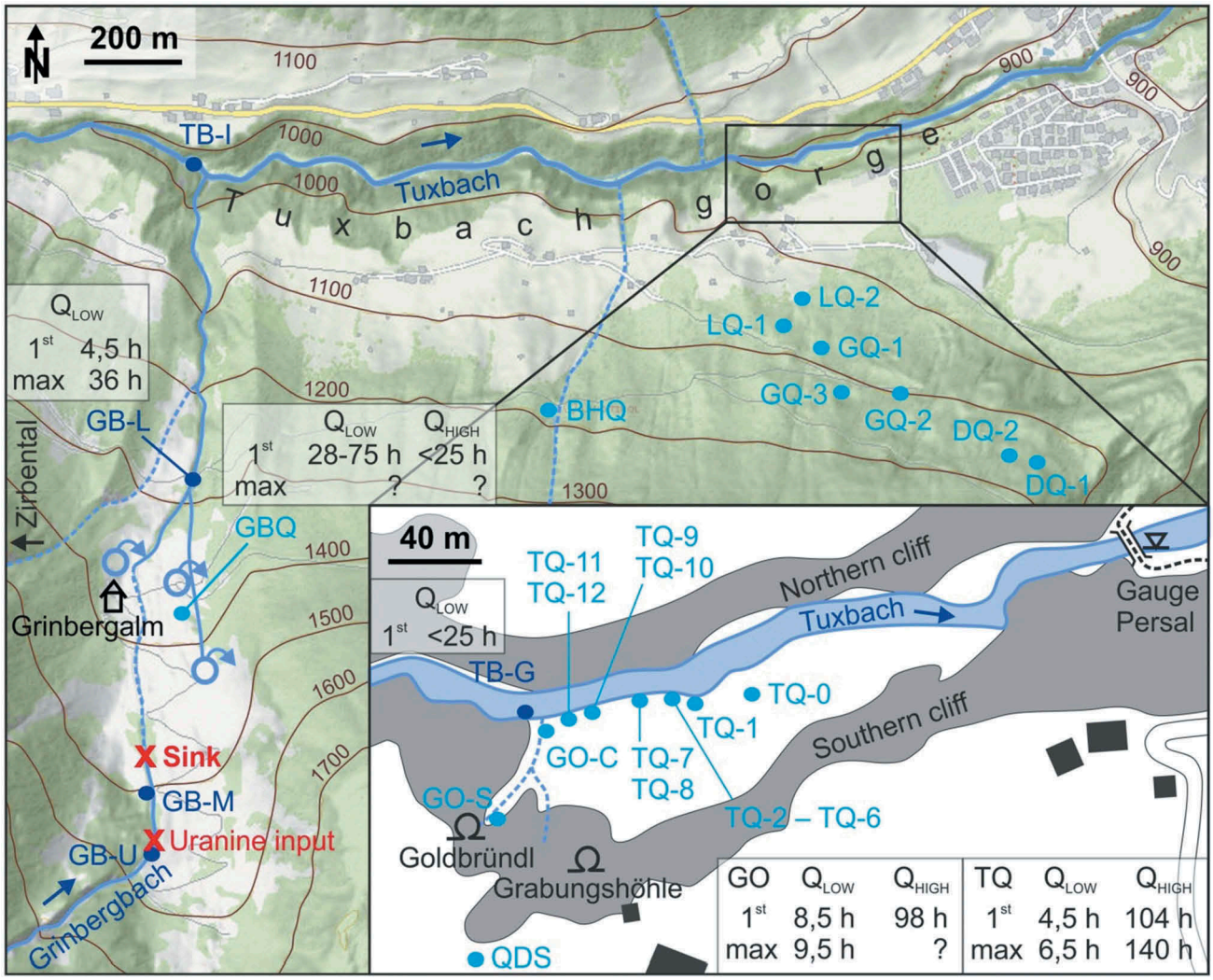

Figure 2. Position plan of the measuring points for both tracer tests: light blue circles indicate springs; dark blue circles creeks. The map background was taken from the Tyrolean Geographic Information System (2019). Overview of the first and maximal uranine transit in the different measuring points during the tracer tests at low (Q_{LOW}) and high (Q_{HIGH}) runoff.

Methods

Tracer test schedule

Two tracer tests were carried out, one at low runoff and one at high runoff. The experiments consisted of three phases (Table 1). In the first phase until the input of uranine, the measuring points were set up and natural backgrounds of relevant parameters, including extinction, water temperature, pH, electrical conductivity, and turbidity, were recorded. During the direct monitoring phase, all measuring points were checked once to several times a day. Important measuring points were sampled at significantly shorter intervals, often several times an hour. During the phase of indirect monitoring, only activated carbon bags and an autosampler were used. Due to the much higher dilution, for the test at high runoff a tenfold higher amount of dye was used.

Monitoring network

The monitoring network included three stations within the Grinbergbach, the Grinbergbachquelle (GBQ), all known springs within the Tuxbach gorge, and eight springs south of Finkenberg (Figure 2, Table 2). In the tracer test at low

Table 1. Schedule for both tracer tests.

	Preparation	Uranine intake	Direct monitoring	Indirect monitoring
Test at low runoff in 2016	4 to 8 September	8 September, 10:30 a.m., 160 g	8 to 14 September	14 September to 11 October
Test at high runoff in 2017	7 to 9 June	9 June, 9:35 a.m., 1.6 kg	9 to 13 June	14 to 29 June

Table 2. List of measuring points.

Measuring point	Abbreviation	Position (UTM 32T)	Altitude (m)
Brunnhausquelle	BHQ	712653; 5225049	1,170
Dornauquelle 1	DQ-1	713642; 5224986	1,131
Dornauquelle 2	DQ-2	713566; 5225017	1,126
Grünbergquelle	GBQ	711849; 5224621	1,380
Grinbergbach—Upper section	GB-U	711859; 5224132	1,553
Grinbergbach—Middle section	GB-M	711850; 5224245	1,502
Grinbergbach—Lower section	GB-L	711931; 5224888	1,273
Goldbründl—Confluence	GO-C	713070; 5225538	897
Goldbründl—Spring	GO-S	713079; 5225494	916
Gamshüttenwegquelle 1	GQ-1	713217; 5225159	1,082
Gamshüttenwegquelle 2	GQ-2	713295; 5225092	1,101
Gamshüttenwegquelle 3	GQ-3	713227; 5225107	1,107
Lampnerquelle 1	LQ-1	713141; 5225259	1,055
Lampnerquelle 2	LQ-2	713170; 5225282	1,039
Quelle in der Seiche	QDS	713049; 5225431	990
Tuxbach—Gorge	TB-G	713066; 5225542	896
Tuxbach—Innerberg	TB-I	711920; 5225522	949
Tuxbachquelle	TQ-0 to TQ-12	713199; 5225543 713108; 5225560	894–901

runoff, TB-I served as a background measuring point and GB-U served as a background measuring point at high runoff in the tracer test. It was possible to sample the previously inaccessible GQ-1 for the tracer test at high runoff. GO-S was installed due to the high discharge of the Goldbründl. The uranine intake on the Grinbergbach was at 711859 E, 5224173 N at an altitude of 1,534 m.

Measurements

Position and weather station

Coordinates and altitudes of the measuring points were measured with GPS devices and checked with the Tyrolean Geographic Information System 3.0 (Tyrolean Geographic Information System 2019). All coordinates are given in WGS 1984, UTM zone 32T; all altitudes are given in meters above the Adriatic Sea.

A weather station was operated from 24 August 2016 to 14 September 2016 and from 28 June 2017 to 30 October 2017 on the Gamshütte at 1,921 m (Figure 1). The weather station (Davies, model Vantage Pro2) records air temperature, air pressure, wind direction, wind speed, precipitation, humidity, and solar radiation.

Uranine

Various fluorescent dyes are widely used in karst hydrology (Goldscheider et al. 2008; Leibundgut, Maloszewski, and Külls 2009). Uranine was used because it can be detected easily and is sufficiently accurate in the field. Due to health concerns, the water management authority did not approve an additional use of rhodamine (cf. Behrens et al. 2001). The quantitative detection of uranine was carried out with two portable fluorometers by Turner Designs (model Aquafluor) at an extinction rate of 515 nm. Multipoint calibration was performed on the devices at a concentration range of 0.1 to 200 µg/L. Water samples were taken for immediate analysis in plastic cuvettes or were filled unfiltered into brown glass bottles and kept protected from light until measurements were performed. Turbid samples were stored until the suspended matter was deposited. Extinction was corrected using formulas from Cao et al. (2017) for pH and from Leibundgut, Maloszewski, and Külls (2009) for water temperature. Consideration of uranine decomposition due to photolysis (Käß 2004) was not necessary, because the superficial flow path was quite short.

In the experiment during high runoff, three autosamplers from Maxx (model P6 L) were placed in GB-M, TQ-1, and TQ-11. The autosamplers were mainly used to collect continuously water samples during the night, which were analyzed the following morning. In addition, the autosamplers were able to take samples from GB-M, TQ-1, and TQ-11 for a few days during the period of indirect monitoring (Table 1).

Activated carbon bags from Provital were applied for the qualitative detection of uranine. Each sachet contained 2.8 g activated carbon with a grain size of 0.5 to 1.0 mm. This brand had performed best in our own laboratory tests. The use of activated carbon is based on a method developed in the Alps by Bauer (1967, 1972) with our own modifications. The activated carbon bags were exposed to 110°C in a drying oven for 24 hours before use. Two activated carbon sachets were simultaneously emplaced for each measuring point. One bag was changed daily during the preparation and direct monitoring periods (Table 1) and served for the detection of the exact day of possible uranine passage. The other bag was exposed to the spring or creek water for several days to a few weeks to detect very low concentrations of uranine and was only exchanged between the direct and indirect monitoring periods. Collected bags were washed as quickly as possible, usually in the afternoon in our improvised laboratory. First, they were dehydrated in a drying oven at 60°C. Then the eluent, which was composed of 12 ml of 96 percent ethanol and 4 ml of 15 percent caustic potash per 5 g of activated carbon, was freshly prepared before use to prevent coloration. Elution was carried out for 30 minutes in a brown tube in a slowly spinning rotator to prevent mechanical comminution of the coal as well as turbidity of the eluate. Organic material attached to the activated carbon grains causes a fluorescence background upon elution, which may remarkably affect the detection of low uranine concentrations (Bauer 1972). This occurred especially with the samples from the Tuxbach. Conclusions of the eluent

extinction on the effective uranine concentration were only qualitatively possible, because the extinction depends on many factors, such as uranine concentration in the water, exposure time, grain size, and amount of activated carbon. The extinction values were corrected for the blank value and the natural background concentration. Results of the activated carbon bags were divided into four categories: no evidence, questionable evidence with minor concentrations, strong evidence, and certain evidence of uranine (Table 3).

Discharge and runoff

Depending on the local conditions, direct or indirect measurement methods (Coldewey and Göbel 2015) were used to determine discharge and runoff. At TQ-1, a hydrometric vane (Ott Hydromet, Germany) was used at an improvised weir. At other Tuxbachquelle outlets, if possible, the outflow was manually diverted, dug, or channeled with material found in situ like pebbles, sand, or moss in order to be able to fill the discharge into measuring cups or plastic bags. Where such an approach was not possible, the discharge was estimated. Spring water and river water were easily distinguishable by measurements of turbidity, temperature, and electrical conductivity.

In addition, two wildlife observation cameras were installed next to TQ-1 and GO-S following the high runoff rate experiment. Pictures taken at regular intervals allowed quantitative estimations of the discharge rates and water turbidity.

Physicochemical parameters

Water temperature and pH were defined at least once a day at all measuring points in order to correct the measured extinction values. Temperature, pH, electrical conductivity (at 25°C), redox potential (E_H), oxygen content, and oxygen saturation were measured at the beginning and end of the tracer tests with devices from WTW (universal pocket meter Multi 340i) and HACH (portable meter HQd). In addition, multiprobe logger systems (Manta Sub2, Eureka Water Probes) were used to survey TQ-1 and GO-A in more detail. Parameters were recorded hourly in TQ-1 and three times a day in GO-A at 8-hour intervals. The turbidity of the Tuxbach and the outlets of the Tuxbachquelle was quantified with a portable turbidimeter from HACH (model 2100Q is).

Hydrochemical parameters

Water samples were collected at the beginning and end of the tracer tests and filled into two bottles of 100 ml each. Samples for cation analysis were acidified with hydrochloric acid to approximately pH 2. The concentrations of sodium (Na^+), potassium (K^+), magnesium (Mg^{2+}), calcium (Ca^{2+}), strontium (Sr^{2+}), ammonium (NH_4^+), nitrite (NO_2^-), nitrate (NO_3^-), phosphate (PO_4^{3-}), sulfate (SO_4^{2-}), fluorine (F^-), chloride (Cl^-), and bromide (Br^-) were analyzed with an ion exchange chromatograph from Metrohm (device 882 Compacts IC plus).

The concentration of bicarbonate (HCO_3^-) was titrated on-site with a digital titrator from HACH (model 16900). The titration sample was buffered with sulfuric acid to pH 4.3, indicated by the color change of Bromcresol green methyl orange ($C_{21}H_{14}Br_4O_5S$, $C_{14}H_{15}N_3O_3S$).

Results

Tracer test at low runoff rate (September and October 2016)

In late summer, runoff from the Grinbergbach varied about 5 L/s and infiltrated completely into the sink. The

Table 3. Qualitative classification of the activated carbon bags of the tracer test at low runoff.

	Short-term activated carbon bags (days in September)					Long-term activated carbon bags	
Measuring point	7–8	8–9	9–10	10–12	12–14	08/09–14/09	14/09–11/10
BHQ		–	–		–	–	–
DQ-1		–			–	–	+
DQ-2		–			–	–	
GBQ		–		+	–	–	++
GB-U		–			–	–	
GO-C	–	–	–	–	–	–	
GQ-1	–			–	–	–	
GQ-2		–	–	–	–	–	–
GQ-3		–	–	–	–	–	
LQ-1		–	–		–	–	–
LQ-2		–	–	–	–	–	+
QDS	–	–	–	–	–	–	–
TB-I	–			–	–	–	
TB-G	–		–	–	–	–	+
TQ-1	–	+	–	–	–	–	++
TQ-2	–	–	–	–	–	–	+
TQ-4	–	–	–	–	–	–	
TQ-10	–	–	–			–	

Note: – = no evidence; + = possible evidence of traces; ++ = strong evidence. Empty fields indicate no sample.

creek bed below was dry from the sink to the Grinbergalm (Figure 2). In the initial test phase, TQ-1 to TQ-5 and TQ-10 were running; all other outlets of the Tuxbachquelle were dry. TQ-10 dried out on 10 September. The water temperatures and electrical conductivities of the Tuxbachquelle outlets were in an identical range (Table 4) and differed significantly from Goldbründl (GO-C) and Tuxbach (TB-I). Turbidity was particularly appropriate to distinguish the clear spring water (0.1 FNU to 4.3 FNU) from the turbid creek water (250 FNU to 410 FNU; Table 4), because the values differed by at least two orders of magnitude. The Goldbründl was almost dry on 14 September and had a discharge rate lower than 0.1 L/s on 11 October. TQ-3, TQ-4, and TQ-5 were dry on 11 October. Table A1 in the Appendix shows the properties of spring waters in comparison to the Grinbergbach.

The blank extinction was 0.2. An extinction rate of up to 0.4 in springs and up to 2.0 in creeks was found before uranine input. These values were considered as natural backgrounds. Noticeable values were detected in almost all monitored outlets of the Tuxbachquelle (TQ-2, TQ-4, and TQ-10) on 8 September (Figure 3), peaking 4½ to 6½ hours after uranine input. A second but lower maximum occurred between 9 and 11 hours after the input. In addition, two elevated values were found in DQ-1 on 9 September: 1.5 at 11:00 a.m. and 0.9 at 2:30 p.m. At all other measuring points no increased extinctions were observed.

Traces of uranine were detected in TQ-1 from 8 to 9 September and in GBQ from 10 to 12 September. Uranine was reliably detected in TQ-1 and GBQ within the second long-term exposure period, and possible uranine traces were found in DQ-1, LQ-2, TB-G, and TQ-2. All other findings were negative.

Table 4. Comparison of selected parameters of the measuring points within the Tuxbach gorge from 8 to 14 September 2016.

Measuring point	*Q* (L/s)	*T* (°C)	pH	κ at 25°C (µS/cm)	Turbidity (FNU)
TQ-1	190–275	6.1–6.5	7.62–8.29	133–152	0.1–2.1
TQ-2	19	6.1–6.4	7.93–8.34	134–153	2.0–2.4
TQ-3	0.2–2.3	6.1–6.9	7.46–8.29	132–152	1.5–3.0
TQ-4	ca. 2	6.1–6.5	7.58–8.35	135–139	1.5–4.3
TQ-5	ca. 100	6.1–6.2	8.20	143	2.1–3.8
TQ-10	<0.05	6.4–6.8	8.21	145–155	4.1
GO-C	0.3–1.9	8.2–10.0	7.98–8.38	169–220	0.7–1.2
TB-G	3,000–3,500	10.5–13.2	8.34–8.39	304–338	250–410

Tracer test at high runoff rate (June 2017)

This tracer test took place after several days of heavy rainfall causing about 30 L/s of runoff from the Grinbergbach. The sink was not able to contain the entire runoff and approximately 5 L/s did overflow.

At the beginning, all known outlets of the Tuxbachquelle were running. TQ-1, TQ-4, TQ-9, TQ-10, TQ-11, and TQ-12 were chosen for regular measurements, because these outlets presented the largest discharge and provided a comprehensive spatial representation (Figure 2, Table 5). For comparison, TQ-0, TQ-3, TQ-5, and TQ-6 were measured sporadically.

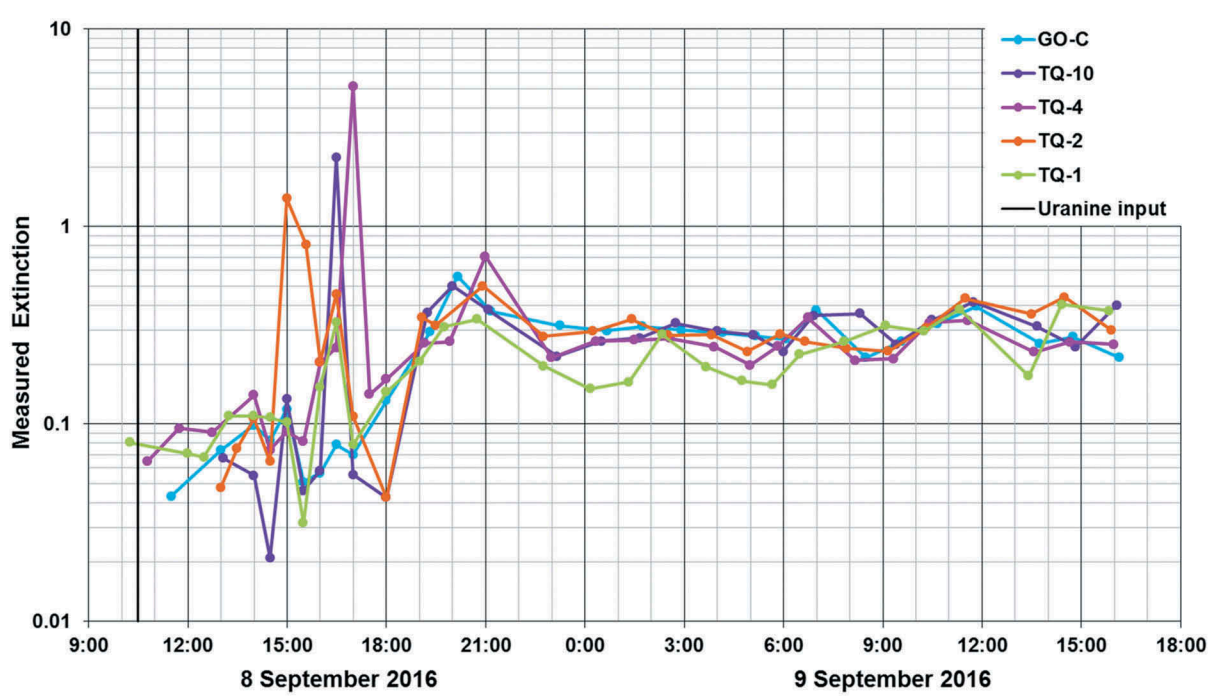

Figure 3. Measured extinctions in the Tuxbach gorge during the first hours of the tracer test at low runoff.

Table 5. Comparison of selected parameters of the measuring points within the Tuxbach gorge from 7 to 29 June 2017.

Measuring point	*Q* (L/s)	*T* (°C)	pH	κ at 25°C (μS/cm)	Turbidity (visual)
TQ-0	0–0.25	5,2	8.25	126	Clear
TQ-1	262–330	5.0–5.5	8.27–8.47	103–138	Clear to slightly muddy
TQ-3	ca. 15	5.0	8.25	112	Clear to slightly muddy
TQ-4		5.0–5.6	8.25–8.36	102–138	Clear to slightly muddy
TQ-5	ca. 110–115	5.0	8.25	112	Clear
TQ-6	ca. 0.25	5.0	8.29	111	Clear
TQ-9	ca. 4–5	4.9–5.4	8.17–8.38	104–138	Clear
TQ-10	ca. 25–30	4.9–5.2	8.16–8.38	104–138	Clear
TQ-11	ca. 44–50	5.0–5.3	8.07–8.31	104–138	Clear
TQ-12	ca. 3–10	4.9–5.3	8.14–8.33	104–138	Clear
GO-S	ca. 0.25–1,000	5.2–5.6	8.15–8.48	106–115	Clear
GO-C		6.1–6.6	8.11–8.20	115–144	Clear
TB-G	5,300–5,700	8.4–12.8	8.17–8.31	245–277	Heavily muddy

Most of the runoff had to be estimated visually because of the elevated discharge rates. TQ-2 could not be investigated at all because this outlet was flooded by the Tuxbach. However, the activity was visible because of the slighter turbidity of the Tuxbach.

There were significant changes in the discharge rates of all outlets of the Tuxbachquelle on direct monitoring days (Table 1). On 10 June all outlets showed a much higher discharge rate than on the previous day, presumably as a result of intense precipitation during the night. Floods repeatedly caused equipment losses during the night from 10 to 11 June and from 11 to 12 June below Goldbründl. During 13 June Goldbründl swelled within several hours from a runlet to a creek discharging in a range of 0.75 to 1 m^3/s.

In GB-L, in the direct outflow of the sink (Figure 2), increased extinctions were noted a few hours after uranine input (Figure 4). Maximum extinction occurred on 11 June, 48½ hours after the input. On 29 June, at the end of the indirect monitoring period, increased extinctions were still measurable in this section of the Grinbergbach. In single measurements for comparison, significantly increased extinctions were detectable from 9 to 11 June in the small creek east of GBQ but not in the GBQ itself.

In contrast, no noticeable elevated extinction was found in any other spring, including the outlets of the Tuxbachquelle, until 13 June. However, using the autosamplers positioned at TQ-1 and TQ-11, uranine passage was detected from 13 to 15 June (Figure 4). Unfortunately, a longer sampling was not possible due

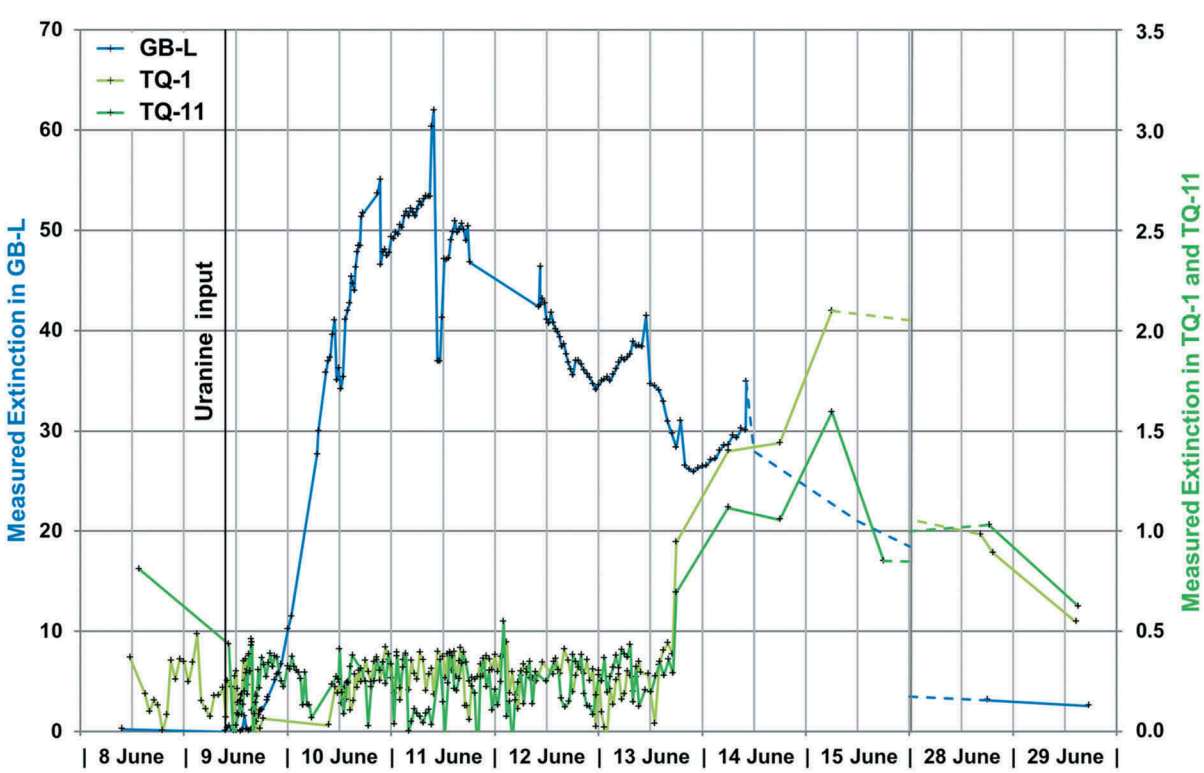

Figure 4. Measured extinctions during the tracer test at high runoff at selected measurement points in June 2017.

to the exhausted batteries. Thus, it is uncertain whether the uranine peak (measured extinctions of 1.59 and 2.10, respectively) took place on 15 June or several days later. This evidence of uranine was not an artifact related to the autosamplers. Increased extensions amounting to up to 0.55 to 1.03 in TQ-1, TQ-11, and GO-S were also detected directly on 28 and 29 June during the final sample collection.

Analysis of the activated carbon bags supported the above results (Table 6). An activated carbon bag placed for comparison between the input position and sink (at GB-S) achieved the largest extinction, followed by the bags from GB-L. Because the Grinbergbach was overflowing the sink, this finding is not surprising. It is rather interesting that the uranine was still detectable for at least four days after its input in the upper part of the Grinbergbach: the last measurement on 14 June resulted in a measured extinction of 34.9 (Figure 4). Traces of uranine reached the Tuxbach gorge (measuring point TB-G; Figure 2) via the superficial flow path on the same day (Table 6). Larger amounts were found in the following days. Traces of uranine were also detectable in GBQ during the same period. Uranine reached Goldbründl (GO-C) for the first time on 11 June and several outlets of the Tuxbachquelle on 12 June and was then detected repeatedly in trace concentrations. In the long-term bags, high extinctions were measured from 13 to 28 June, providing reliable proof of uranine. In addition, single long-term bags in DQ-1, GQ-1, GQ-2, LQ-2, and QDS may indicate traces of uranine.

A wet landslide, triggered by a half-hour summer thunderstorm with hail, occurred on the evening of 24 June. According to local witnesses, it was the fiercest mudflow during the last 75 years in the Grinberg area. The mudflow initiated from a steep, snow-covered section of the northeastern flank of the Grinbergspitze at about 2,240 m and descended following the flow path of the Grinbergbach to the Tuxbach. The creek bed of the Grinbergbach was completely reworked and boulders of up to a few meters were transported. In doing so, the autosampler positioned at GB-L was destroyed and lost.

Additional investigations (July and August 2017)

In order to examine the impact of the mudflow on the sink hole, further investigations were performed in July and August at TQ-1 (Figure 5) and GO-A (Figure 6). It became evident that the Tuxbachquelle responds within a few hours to precipitation events: the discharge increases significantly, electrical conductivity decreases, and temperature increases slightly. These effects coincide temporarily with maximum precipitation and a temporary turbidity. Water temperature rises slightly and electrical conductivity rises significantly during longer dry periods. A typical increase is within the range of 45 to 80 µS/cm.

Table 6. Qualitative classification of the activated carbon bags of the tracer test at high runoff.

	Short-term activated carbon bags (days in June)					Long-term activated carbon bags (days in June)	
Measuring point	8–9	9–10	10–11	11–12	12–13	8–13	13–28
BHQ	–	–	–	–	–	–	
DQ-1	–	–	–	–	–	+	
DQ-2	–	–	–	–	–	–	
GBQ	–	+	+	+	+	+	++
GB-U			–	()	–	–	()
GB-M		+++					
GB-L		+++	+++	+++	+++	+++	()
GO-C	–	–	+	()	+	+	+++
GQ-1					–		+
GQ-2	–	–	–	–	–	–	+
GQ-3	–	–	–	–	–	–	–
LQ-1	–	–	–	–	–	–	–
LQ-2	–	–	–	–	–	–	+
QDS	–	–	–	–	–	–	+
TB-G	–	+	++	+	++	++	++
TQ-1	–	–	–	+	+	+	+
TQ-4	–	–	–	–	–	+	+++
TQ-9	–	–	–	–	+	+	++
TQ-10	–	–	–	+	+	+	+++
TQ-11	–	–	–	+	+	+	+++
TQ-12	–	–	–	+	+	+	+++

Note: – = no evidence; + = possible evidence of traces; ++ = strong evidence; +++ = certain evidence of uranine; () = damage or loss of samples due to floodwater or mudflow. Empty fields indicate no sample.

Goldbründl shows a pattern of daily temperature oscillation, typically within the range of 0.8°C to 1.2° C. Maxima take place shortly after midday and minima occur around midnight. Heavy rainfall events interrupt this pattern (Figure 6). As in the Tuxbachquelle, temperature and electrical conductivity drop within a few hours after the beginning of precipitation events. In dry periods, the original conductivity recovers within a few hours, whereas the water temperature rises for days. In summary, Goldbründl is much more sensitive to weather than Tuxbachquelle.

Discussion

Uranine recovery

The recovery rate for the test during high runoff was 106 percent of the amount of uranine used. This calculation includes an extinction correction for pH, water temperature, and natural background. Because discharge or runoff was often estimated, this inaccuracy might be the reason for the apparently too high recovery rate. Seventy-seven percent of the uranine passed the Grinbergbach below the sink at measuring point GB-L, and 29 percent took the underground flow path and reached the Tuxbachquelle or Goldbründl. Despite the uncertainties regarding the recovery rate, it can be assumed that the measuring network is complete and that uranine did not leak at unknown locations.

Residence time and average flow velocity

Including the vertical height, the direct flow distance between the sink and Tuxbachquelle or Goldbründl is 1,920 m. The distance between the sink and measuring point GB-L is 570 m. The flow time between input location and sink (distance 150 m) was neglected, because the flow time was only a few minutes.

For the tracer test at low runoff, the uranine peak concentration reached different outlets of the Tuxbachquelle after 4½ to 6½ hours (Figure 2). These times are similar to those of the observed response of the Tuxbachquelle and Goldbründl to heavy precipitation of a few hours (Figures 5 and 6). This results in an average flow velocity of 0.08 to 0.12 m/s or 300 to 425 m/h. In the tracer test at low runoff, the maximum uranine concentration arrived much later in the Tuxbachquelle; that is, 140½ hours after the input. This

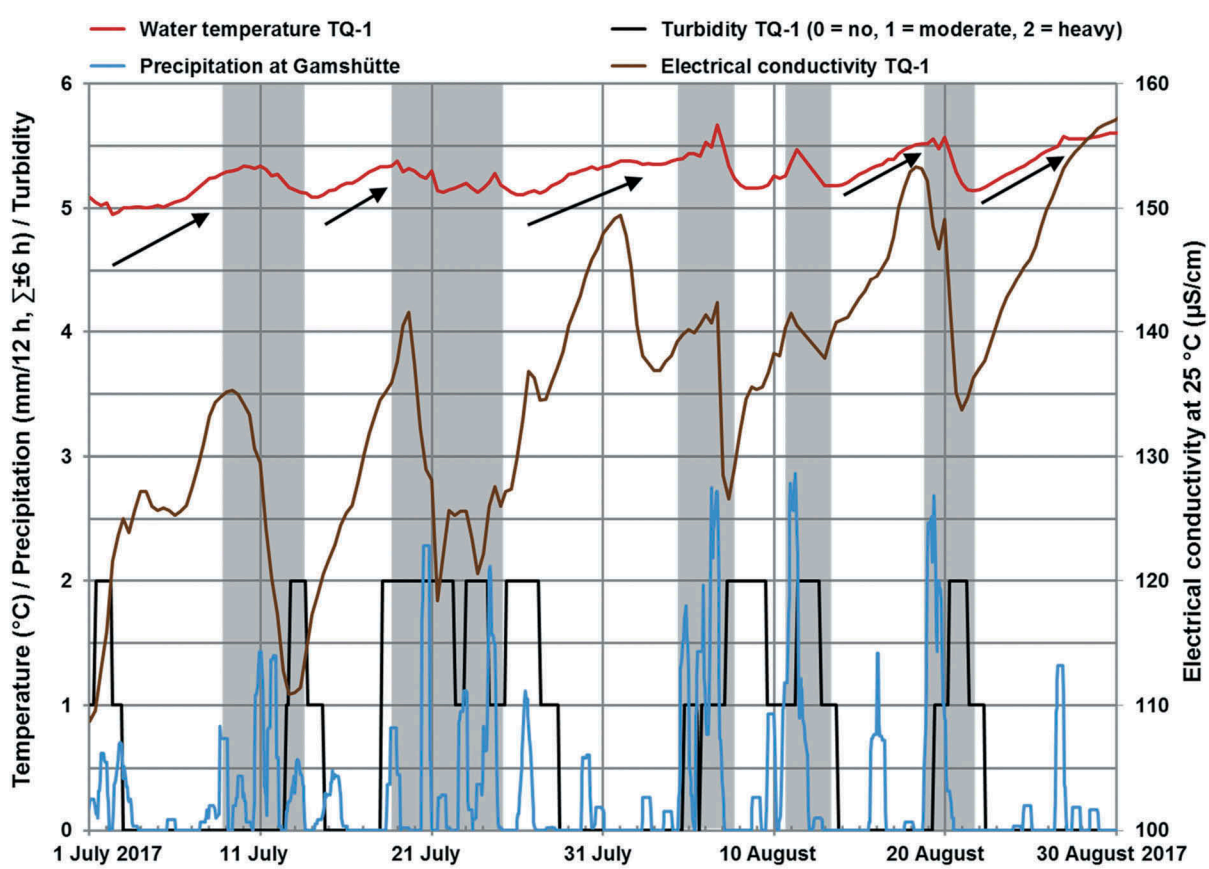

Figure 5. Water temperature, electrical conductivity, and quantitative estimated turbidity at the Tuxbachquelle (outlet TQ-1) in comparison to precipitation at Gamshütte. Important precipitation events are marked with a gray background.

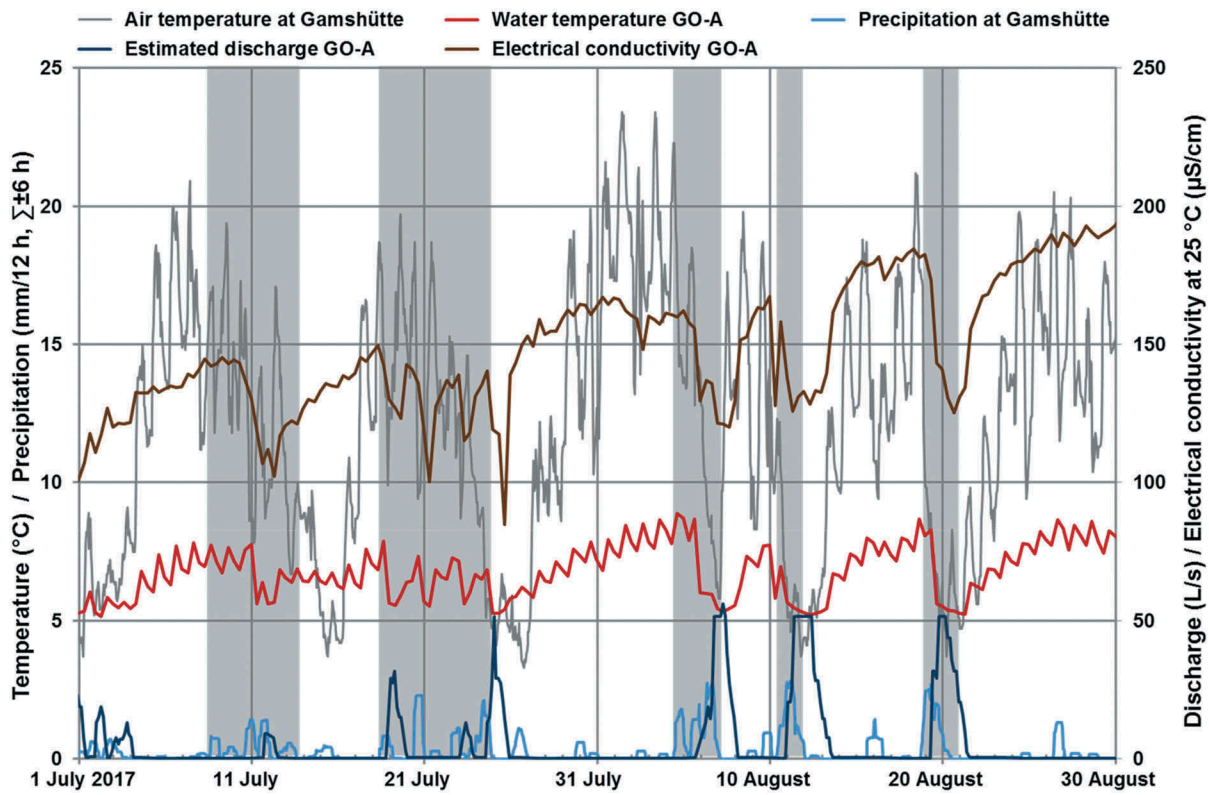

Figure 6. Water temperature, electrical conductivity, and estimated discharge based on photos at Goldbründl (measuring point GO-A) in comparison to precipitation at Gamshütte. Important precipitation events are marked with a gray background.

resulted in an average flow velocity of $4 \cdot 10^{-3}$ m/s or 14 m/h. Interestingly, the average flow velocity between the sink and GB-L was very similar, amounting to $3 \cdot 10^{-3}$ m/s or 12 m/h. The maximum uranine concentration occurred in GB-L 48½ hours after the input (Figure 2).

The residence time and average flow velocity between the sink and Tuxbachquelle or Goldbründl were highly variable; that is, they were 25 times longer at high runoff than at low runoff. The high runoff, caused by the intense rainfalls at the beginning of June 2017, might have resulted in saturation and temporary storage of infiltrated water within the karst system. The water was retained for days at narrow passages, resulting in a significant delay of the uranine transit. The flow velocities in the karst at high runoff were connatural to a flow velocity of $1.7 \cdot 10^{-4}$ m/s obtained in karstified and saturated parts of the Hochstegen Formation below Finkenberg at a depth of 340 m (Lehr and Sass 2014).

Most of the uranine did not reach the lower section of the Grinbergbach (GB-L) via the superficial flow path but underground through the quaternary deposits. This estimation coincides with the observation during high runoff in June 2017. About 85 percent of the Grinbergbach discharge infiltrated the sink and 15 percent of the volume followed the creek bed.

Karstification of the Hochstegen Formation

Assuming the karst system to be completely water saturated at the moment of uranine infiltration and the runout to take place exclusively at the Tuxbachquelle and the Goldbründl, a void volume of 190,000 to 330,000 m^3 was estimated for the Hochstegen Formation between the sink and Tuxbach gorge, depending on supposed discharge rates. Grabungshöhle and Goldbründl Cave are therefore manifestations of a much larger karst system.

Catchment area

The Austrian Hydrographic Service runs three precipitation measurement stations in the vicinity of Finkenberg (Lanersbach, #102 640; Geschößwand, #103 192; and Ginzling, #102 632). From 2010 to 2014, the mean precipitation was 1,290 mm (AHS 2019). According to BLFUW (2013), the potential evaporation on the north side of the Alpine main ridge is in the range of 294 to 469 mm at an altitude of 1,350 to 1,940 m. Based on data for one year, the storage change is negligible, so it was assumed that the mean water supply is 0.91 m/a. Thus, a 2.4 km^2 catchment area is required for a discharge of 70 L/s and an area of about 7.0 km^2 for 200 L/s.

The geographic catchment area of the sink, assessed over 1.9 km^2 (Figure 1), is apparently too small to solely feed the discharge of the Tuxbachquelle, despite taking into account contributions of melting dead ice and a cirque glacier to the runoff of the Grinbergbach. The catchment area of the Tuxbachquelle possibly extends to Zirbental and Brunnhauswald. This would increase the catchment area to 4.2 km^2, although previous field observations did not find evidence of a contribution of the Brunnhauswald area. An extension of the catchment area, exceeding the Tux Main Ridge in the southern or eastern direction (Figure 1), can be dismissed for morphological, geological, and hydrogeological reasons. The geometry of fabric elements or tectonic features does not fit to be considered as hydraulically effective pathways crossing the Tux Main Ridge in this area (Behrmann and Frisch 1990; Lammerer and Weger 1998). Nappe thrust faults, the Olperer Shear Zone, and the foliation of the Ahorn Gneiss are all roughly southwest to northeast. The terrain drops steeply toward the Zemmtal on the other side of the ridge. Drainage takes places mostly overground toward the Zemmbach because the Ahorn Gneiss can hardly absorb precipitation. At the Gamsberg, a glacially smoothed high elevated flat (Wirsig et al. 2016), a mountain splitting caused eleven mostly west–east aligned grooves up to 500 m long and up to 12 m deep, which also dewater to the Zemmbach.

In June 2017, the upper Grinbergbach (measuring point GB-U) had temperatures of 7.5°C to 10.1°C, whereas the Tuxbachquelle had temperatures of 4.9°C to 5.6°C. This relatively low temperature range gives strong evidence that a significant amount of the discharge originates from higher altitudes and/or rock glaciers (Krainer and Mostler 2002). Considering the water balance and water temperature, it is likely that the catchment area of the Tuxbachquelle extends in the strike of the Hochstegen Formation to the southwest (Figure 1). It drains rock glaciers within the Elskar and the Lange Wand Kar area and conceivably other cirques further west (Kogler 2018). As the existence of several caves demonstrates, the Hochstegen Formation is karstified there (Spötl 2009). The significantly lower density of surface water compared to the Ahorn Gneiss at the other side of the Tux Main Ridge supports this finding. In a field of roughly 700 to 100 m at the lower end of the Lange Wand Kar rock glacier, we found twelve sinks and six dolines (cf. Kogler 2018) that possibly feed the Tuxbachquelle. Both Elskar rock glaciers are hardly accessible and therefore only a few sinks have been found so far. The catchment area of the sink, Zirbental, Elskar, and Lange Wand Kar, adds up to 6.4 km^2. This extension could explain the observed discharge rates and temperatures at the Tuxbachquelle. Hydrological studies in other Alpine regions showed that rock glaciers can impact the water quality extensively and can yield a base runoff of 70 to 100 L/s during summer months (Nickus et al. 2015; Thies et al. 2013, 2017; Engel et al. 2019).

Conclusion

All outlets of the Tuxbachquelle had identical hydrochemical and physicochemical properties and can therefore be classified as a spring group. Uranine was detected in several active outlets. Thus, a hydraulic connection between the Tuxbachquelle and the sink on the Grinbergalm is proven. The Tuxbachquelle is a karst spring with variable discharge in the range of about 70 to 200 L/s. During or after precipitation events, discharge can increase up to 500 L/s. Only outlet TQ-1 is perennial; all other outlets are gradually activated with rising runoff rates.

In the Goldbründl, uranine was detected both by direct measurements and by the activated carbon bags, proving a hydraulic connection to the sink on the Grinbergalm as well. The measuring point at the spring (GO-S) is much more suitable for investigations than the one at the confluence in the Tuxbach (GO-C). Despite the short flow path, relevant parameters change due to contact with the air and the inflow of a small intermittent stream. The Goldbründl is an intermittent karst spring. For most of the year, there is a rather low (<0.1 L/s) or even no discharge. After heavy rainfall, the discharge increases within a few hours and can apparently reach 500 L/s. Goldbründl is very similar to the Tuxbachquelle regarding hydrochemical and physicochemical properties. Therefore, it can be considered as an elevated outlet of the Tuxbachquelle.

Low uranine concentrations could also be detected in the Grünbergquelle by means of activated carbon bags in both tracer tests. The Grünbergquelle is considered a pocket spring, fed from the quaternary deposits in the upper part of the Grinbergalm (Figure 1). The filtrate of the sink crosses the catchment area, causing the spring to be a mixture of infiltrated Grinbergbach water and vadose water.

No significant uranine signal was detected at all other monitored springs southwest of Finkenberg. Therefore, there is no evidence of further hydraulic connections from the sink. Nevertheless, noticeable extinctions were derived from single activated carbon bags in DQ-1 and LQ-2 in 2016 and in GQ-1, GQ-2, and QDS in 2017. It is assumed that naturally occurring organic material in the spring water, instead of the

applied uranine, was responsible for the extinction, because (1) these findings were not reproducible, (2 neighboring springs were not affected, and (3) the extinctions were above the natural background values, though only slightly.

Outlook

Stevanović (2019) estimated how climate change, population growth, and other factors will impact karst aquifers suitable for water supply. On a global perspective, only a minor part of annually renewable karstic groundwater is currently exploited, resulting in a large potential. Our study is a local example of how a study could be carried out to investigate such unused water resources. The discharge of the Tuxbachquelle is sufficient to supply Finkenberg. Surveyed hydrochemical and physicochemical parameters fulfill the requirements of the Austrian Drinking Water Regulation (RIS 2019). Before its use as drinking water, microbiological examinations and the definition of a spring reserve, considering the findings presented here, are essential. It might be necessary to restrict the alpine pasture at the Grinbergalm. For a better evaluation of the catchment area of the Tuxbachquelle, further field observations and investigations are required. Firstly, the assumed hydraulic connection to the west should be verified by means of tracer tests. Secondly, in the case of positive findings, the influence of rock glaciers on water quality should be examined in more detail. In order to reduce the uncertainties of the calculations presented here, the construction of weirs at the Grinbergbach and the outlets of the Tuxbachquelle is required for more accurate runoff determination. Due to the proven karstification of the Hochstegen Formation, karst cavities and considerable water invasion will impede the ongoing tunneling.

Acknowledgments

Julian Formhals, Christopher Hesse, Meike Hintze, Hung Pham, Dirk Scheuvens, Gaby Schubert, Rainer Seehaus, Franziska Stemke, and Bastian Welsch helped with tracer tests. Participants of the field exercise “Hauptgeländeübung II 2016” collected samples during the tracer test at low runoff. Data from the gauge Persal were provided by the Hydrographical Service of Tyrol and the gauge’s operator, the Verbund Hydro Power Ltd. Comments from an anonymous reviewer and the editor significantly improved the article.

Disclosure statement

No potential conflict of interest was reported by the authors.

Funding

The publication fee was covered by the German Research Foundation (DFG) and the Open Access Publishing Fund of Technische Universität Darmstadt.

ORCID

Rafael Schäffer http://orcid.org/0000-0002-9717-6496

References

AHS (Austrian Hydrographic Service). Bundesministerium Nachhaltigkeit und Tourismus. Accessed May 10, 2019. http://ehyd.gv.at/#.

Auer, I., R. Böhm, A. Jurkovic, W. Lipa, A. Orlik, R. Potzmann, W. Schöner, M. Ungersböck, C. Matulla, K. Briffa, et al. 2007. HISTALP - historical instrumental climatological surface time series of the Greater Alpine Region. *International Journal of Climatology* 27:17–46. doi:10.1002/(ISSN)1097-0088.

Bauer, F. 1967. Erfahrungen beim Uraninnachweis mit Aktivkohle. *Steirische Beiträge zur Hydrogeologie* 1966/67:169–78.

Bauer, F. 1972. Weitere Erfahrungen beim Uraninnachweis mit Aktivkohle. *Geologisches Jahrbuch* C2:19–27.

Behrens, H., U. Beims, H. Dieter, G. Dietze, T. Eikmann, T. Grummt, H. Hanisch, H. Henseling, W. Käß, H. Kerndorff, et al. 2001. Toxicological and ecotoxicological assessment of water tracers. *Hydrogeology Journal* 9:321–25. doi:10.1007/s100400100126.

Behrmann, J. H., and W. Frisch. 1990. Sinistral ductile shearing associated with metamorphic decompression in the Tauern Window, Eastern Alps. *Jahrbuch der Geologischen Bundesanstalt* 100:135–46.

BLFUW (Bundesministerium für Land- und Forstwirtschaft). 2012. Wasserverbrauch und Wasserbedarf – Auswertung empirischer Daten zum Wasserverbrauch. Bundesministerium für Land- und Forstwirtschaft, 35 p., Umwelt und Wasserwirtschaft, Wien. doi:10.1094/PDIS-11-11-0999-PDN.

BLFUW (Bundesministerium für Land- und Forstwirtschaft). 2013. Hydrographisches Jahrbuch von Österreich, 119. Band 2011. Wasserverbrauch und Wasserbedarf – Auswertung empirischer Daten zum Wasserverbrauch, 967 p., Bundesministerium für Land- und Forstwirtschaft, Umwelt und Wasserwirtschaft, Wien.

Brighenti, S., M. Tolotti, M. C. Bruno, M. Engel, G. Wharton, L. Cerasino, V. Mair, and W. Bertoldi. 2019. After the peak water: The increasing influence of rock glaciers on alpine river systems. *Hydrological Processes* 33:2804–23. doi:10.1002/hyp.v33.21.

Brunetti, M., G. Lentini, M. Maugeri, T. Nanni, I. Auer, R. Böhm, and W. Schöner. 2009. Climate variability and change in the Greater Alpine Region over the last two centuries based on multi-variable analysis. *International Journal of Climatology* 29:2197–225. doi:10.1002/joc.1857.

Brunetti, M., M. Maugeri, T. Nanni, I. Auer, R. Böhm, and W. Schöner. 2006. Precipitation variability and changes in the greater Alpine region over the 1800–2003 period.

Journal of Geophysical Research 111:D11107. doi:10.1029/2005JD006674.

Cao, V., M. Schaffer, Y. Jin, and T. Licha. 2017. Preservation of commonly applied fluorescent tracers in complex water samples. *Grundwasser* 22:127–33. doi:10.1007/s00767-017-0356-1.

Christian, E., and C. Spötl. 2010. Karst geology and cave fauna of Austria: A concise review. *International Journal of Speleology* 39:71–90. doi:10.5038/1827-806X.

Coldewey, W. G., and P. Göbel. 2015. *Hydrogeologische Gelände- und Kartiermethoden*, 180 p. Berlin: Springer Spektrum.

Colombo, N., F. Salerno, S. Gruber, M. Freppaz, M. Williams, S. Fratianni, and M. Giardino. 2018. Review: Impacts of permafrost degradation on inorganic chemistry of surface fresh water. *Global and Planetary Change* 162:69–83. doi:10.1016/j.gloplacha.2017.11.017.

Engel, M., D. Penna, G. Bertoldi, G. Vignoli, W. Tirler, and F. Comiti. 2019. Controls on spatial and temporal variability in streamflow and hydrochemistry in a glacierized catchment. *Hydrology and Earth System Sciences* 23:2041–63. doi:10.5194/hess-23-2041-2019.

Fischer, A., B. Seiser, M. Stocker Waldhuber, C. Mitterer, and J. Abermann. 2015. Tracing glacier changes in Austria from the Little Ice Age to the present using a lidar-based high-resolution glacier inventory in Austria. *The Cryosphere* 9:753–66. doi:10.5194/tc-9-753-2015.

Fliegl, M. 2017. Projekt Unterer Tuxbach. Proceedings of the 20th Vilser Baustofftag, Reutte, Austria.

Frisch, W. 1968. Zur Geologie des Gebietes zwischen Tuxbach und Tuxer Hauptkamm bei Lanersbach (Zillertal, Tirol). *Mitteilungen der Gesellschaft der Geologie- und Bergbaustudenten Österreichs* 18:287–336.

Frisch, W. 1980. Post-Hercynian formations of the western Tauern window: Sedimentological features, depositional environment, and age. *Mitteilungen der Österreichischen Geologischen Gesellschaft* 71/72:49–63.

Gobiet, A., S. Kotlarski, M. Beniston, G. Heinrich, J. Rajczak, and M. Stoffel. 2014. 21st century climate change in the European Alps - A review. *Science of the Total Environment* 493:1138–51. doi:10.1016/j.scitotenv.2013.07.050.

Goldscheider, N., J. Meiman, M. Pronk, and C. Smart. 2008. Tracer tests in karst hydrogeology and speleology. *International Journal of Speleology* 37:27–40. doi:10.5038/1827-806X.

Gross, G. 1987. Der Flächenverlust der Gletscher in Österreich 1850-1920-1969. *Zeitschrift für Gletscherkunde und Glazialgeologie* 2:131–41.

Huss, M. 2011. Present and future contribution of glacier storage change to runoff from macroscale drainage basins in Europe. *Water Resources Research* 47:W07511. doi:10.1029/2010WR010299.

Käß, W. 2004. *Geohydrologische Markierungstechnik*. Lehrbuch der Hydrogeologie Band 9, 557 p. Berlin: Gebrüder Borntrager.

Kobierska, F., T. Jonas, M. Zappa, M. Bavay, J. Magnusson, and S. M. Bernasconi. 2013. Future runoff from a partly glacierized watershed in Central Switzerland: A two-model approach. *Advances in Water Resources* 55:204–14. doi:10.1016/j.advwatres.2012.07.024.

Kogler, T. 2018. Quartärgeologie und Permafrost (Blockgletscher) am Tuxer Hauptkamm (Zillertaler Alpen, Tirol, Österreich). Unpublished MS thesis, Leopold-Franzens-Universität Innsbruck, 144 p.

Krainer, K., and W. Mostler. 2002. Hydrology of active rock glaciers: Examples from the Austrian Alps. *Arctic, Antarctic, and Alpine Research* 34:142–49. doi:10.1080/15230430.2002.12003478.

Krainer, K., and M. Ribis. 2012. A rock glacier inventory of the Tyrolean Alps (Austria). *Austrian Journal of Earth Sciences* 105:32–47.

Lambrecht, A., and M. Kuhn. 2007. Glacier changes in the Austrian Alps during the last three decades derived from the new Austrian glacier inventory. *Annals of Glaciology* 46:177–84. doi:10.3189/172756407782871341.

Lammerer, B., and M. Weger. 1998. Footwall uplift in an orogenic wedge: The Tauern Window in the Eastern Alps of Europe. *Tectonophysics* 285:213–30. doi:10.1016/S0040-1951(97)00272-2.

Lehr, C., and I. Sass. 2014. Thermo-optical parameter acquisition and characterization of geologic properties: A 400-m deep BHE in a karstic alpine marble aquifer. *Environmental Earth Sciences* 72:1403–19. doi:10.1007/s12665-014-3310-x.

Leibundgut, C., P. Maloszewski, and C. Külls. 2009. *Tracers in hydrogeology*, 415 p. Chichester: Wiley-Blackwell.

Nickus, U., H. Thies, and K. Krainer. 2015. Hydrologie und Wasserchemie von Blockgletscherbächen. *Geo.Alp* 12:151–62.

Pröbstl, U., and B. Damm, eds. 2009. *Wahrnehmung und Bewertung von Naturgefahren als Folge von Gletscherschwund und Permafrostdegradation in Tourismusdestinationen am Beispiel des Tuxer Tals (Zillertaler Alpen/Österreich)*, 51 p. Wien: Universität für Bodenkultur.

Rajczak, J., P. Pall, and C. Schär. 2013. Projections of extreme precipitation events in regional climate simulations for Europe and the Alpine Region. *Journal of Geophysical Research: Atmospheres* 118:3610–26.

RIS (Federal Justice Information System). Federal ministry for digital and economic affairs. Accessed June 3, 2019. https://www.ris.bka.gv.at/GeltendeFassung.wxe?Abfrage=BundesnormenandGesetzesnummer=20001483.

Saidi, H., C. Dresti, D. Manca, and M. Ciampittiello. 2018. Quantifying impacts of climate variability and human activities on the streamflow of an Alpine river. *Environmental Earth Sciences* 77:690. doi:10.1007/s12665-018-7870-z.

Sass, I., C.-D. Heldmann, and C. Lehr. 2016. Exploitation of a marble karst reservoir for a medium deep borehole heat exchange system in Tux, Tyrol. *Grundwasser* 21:137–45. doi:10.1007/s00767-016-0327-y.

Sass, I., C.-D. Heldmann, and R. Schäffer. 2016. Exploration and monitoring for geothermal exploitation of an Alpine karst aquifer, Tux valley, Austria. *Grundwasser* 21:147–56. doi:10.1007/s00767-015-0312-x.

Schäffer, R., I. Sass, C.-D. Heldmann, and D. Scheuvens. 2018. Geothermal drilling in an Alpine karst aquifer and its impact on downstream springs – A case study from Finkenberg, Tyrol, Austria. *Acta Carsologica* 47:139–51. doi:10.3986/ac.v47i2-3.4963.

Schwendiger, G., and P. Pindur. 2013. Die Entwicklung der Gletscher im Zemmgrund, Zillertaler Alpen (Österreich), seit dem Hochstand in der Mitte des 19. Jahrhunderts – Längenänderung, Flächen- und Volumenverlust, Schnee

grenzanstieg. *Zeitschrift für Gletscherkunde und Glazialgeologie* 47/48:63–90.

Spötl, C. 2009. Höhlen im Gebiet des Höllensteins, Tuxertal (Tirol). *Höhlenkundliche Mitteilungen* 61:7–16.

Spötl, C., L. Plan, and E. Christian. 2016. *Höhlen und Karst in Österreich*, 752p. Linz: Oberösterreichisches Landesmuseum.

Spötl, C., and A. Schiffmann. 2014. Zwei aktive Kleinhöhlen in der Klamm des Tuxbaches in Finkenberg. *Höhlenkundliche Mitteilungen* 66:19–22.

Stevanović, Z. 2019. Karst waters in potable water supply: A global scale overview. *Environmental Earth Sciences* 78:662. doi:10.1007/s12665-019-8670-9.

Thiele, O. 1976. Der Nordrand des Tauernfensters zwischen Mayrhofen und Inner Schmirn (Tirol). *Geologische Rundschau* 65:410–21. doi:10.1007/BF01808473.

Thies, H., U. Nickus, R. Tessadri, P. Tropper, and K. Krainer. 2017. Peculiar arsenic, copper, nickel, uranium, and yttrium-rich stone coatings in a high mountain stream in the Austrian Alps. *Austrian Journal of Earth Sciences* 110:7.

Thies, H., U. Nickus, M. Tolotti, R. Tessadri, and K. Krainer. 2013. Evidence of rock glacier melt impacts on water chemistry and diatoms in high mountain streams. *Cold Regions Science and Technology* 96:77–85. doi:10.1016/j.coldregions.2013.06.006.

Tyrolean Geographic Information System. Accessed May 10, 2019. https://www.tirol.gv.at/statistik-budget/tiris/ Government of Tyrol.

Wagner, T., M. Themeßl, A. Schüppel, A. Gobiet, H. Stigler, and S. Birk. 2017. Impacts of climate change on stream flow and hydro power generation in the Alpine region. *Environmental Earth Sciences* 76:4. doi:10.1007/s12665-016-6318-6.

Winkler, G., T. Wagner, M. Pauritsch, S. Birk, A. Kellerer-Pirklbauer, R. Benischke, A. Leis, R. Morawetz, M. G. Schreilechner, and S. Hergarten. 2016. Identification and assessment of groundwater flow and storage components of the relict Schöneben Rock Glacier, Niedere Tauern Range, Eastern Alps (Austria). *Hydrogeology Journal* 24:937–53. doi:10.1007/s10040-015-1348-9.

Wirsig, C., J. Zasadni, M. Christl, N. Akçar, and S. Ivy-Ochs. 2016. Dating the onset of LGM ice surface lowering in the High Alps. *Quaternary Science Reviews* 143:37–50. doi:10.1016/j.quascirev.2016.05.001.

Appendix

Table A1. Chemical properties of Grinbergbach at low runoff compared to spring water at the beginning and end of the tracer test. Samples taken in September 2016.

	Measuring point							
	GB-U	GBQ	GBQ	BHQ	BHQ	QDS	QDS	
Date	05/09	05/09	14/09	05/09	14/09	04/09	14/09	
T (°C)	10.8	5.9	6.0	7.0	6.7	11.2	9.2	
κ at 25°C (µS/cm)	76	51	52	114	115	246	252	
pH	7.87	7.57	7.09	7.66	7.18	7.52	7.24	
E_H (mV)	304	348	335	337	314	299	333	
O_2 content (mg/L)	9	10	11	10	10	8	9	
O_2 saturation (%)	101	99	101	95	96	88	89	
Q (L/s)	ca. 5	1.32	0.50	1.53	1.20	0.54	0.25	
Na^+ (mg/L)	0.01	0.32	0.28	0.88	0.97	3.46	3.14	
NH_4^+ (mg/L)	<0.01	0.02	0.04	<0.01	<0.01	<0.01	<0.01	
K^+ (mg/L)	0.44	0.76	0.73	1.20	1.21	2.57	2.44	
Mg^{2+} (mg/L)	2.05	0.88	0.85	2.30	2.32	4.31	4.32	
Ca^{2+} (mg/L)	12.8	8.65	8.75	19.3	19.5	44.5	44.8	
Sr^{2+} (mg/L)	<0.1	<0.1	<0.1	0.18	0.15	0.19	0.22	
F^- (mg/L)	0.02	0.03	0.03	0.07	0.06	0.05	0.05	
Cl^- (mg/L)	0.50	0.72	0.12	0.75	0.72	6.74	6.53	
NO_2^- (mg/L)	0.01	<0.01	< 0.01	0.01	<0.01	<0.01	<0.01	
Br^- (mg/L)	0.09	0.08	0.06	0.13	0.11	0.37	0.21	
NO_3^- (mg/L)	0.98	1.89	1.78	1.69	3.57	7.81	7.52	
PO_4^{3-} (mg/L)	0.09	0.09	0.06	0.09	0.07	0.04	0.05	
SO_4^{2-} (mg/L)	1.82	2.46	2.50	5.11	5.11	3.32	3.43	
HCO_3^- (mg/L)	46.4	28.1	28.1	65.9	65.9	149	142	
TDS (mg/L)	65.2	44.0	43.3	97.6	99.7	222	214	
Δ ion balance (%)	−1.63	−5.16	−1.48	−1.31	−2.40	−1.42	3.32	
Measuring point	GQ-2	GQ-2	GQ-3	GQ-3	LQ-1	LQ-1	LQ-2	LQ-2
Date	06/09	14/09	06/09	14/09	07/09	14/09	07/09	14/09
T (°C)	7.1	7.5	7.8	8.0	8.3	9.1	9.4	10.5
κ at 25°C (µS/cm)	122	127	145	147	133	137	82	86
pH	8.01	7.41	7.87	7.53	7.86	7.53	7.82	7.24
E_H (mV)	307	315	316	311	347	314	366	307
O_2 content (mg/L)	10	10	8	9	11	10	10	10
O_2 saturation (%)	92	93	80	85	100	99	101	100
Q (L/s)	0.63	0.60	0.06	0.05	0.22	0.05	0.16	0.07
Na^+ (mg/L)	1.20	1.12	1.58	1.41	1.21	1.08	1.21	1.26
NH_4^+ (mg/L)	<0.01	<0.01	0.01	0.02	<0.01	<0.01	0.02	<0.01
K^+ (mg/L)	1.30	1.47	1.59	1.64	1.46	1.47	1.09	1.09
Mg^{2+} (mg/L)	2.05	2.50	4.31	4.45	2.82	2.77	2.10	2.25
Ca^{2+} (mg/L)	21.5	22.2	22.2	22.8	23.1	23.8	11.8	12.8
Sr^{2+} (mg/L)	0.22	0.21	0.30	0.29	0.13	<0.1	0.14	0.13
F^- (mg/L)	0.07	0.07	0.09	0.08	0.09	0.09	0.08	0.08
Cl^- (mg/L)	0.49	0.62	0.49	0.40	0.40	0.54	0.40	1.02
NO_2^- (mg/L)	<0.01	<0.01	<0.01	<0.01	0.01	<0.01	<0.01	0.07
Br^- (mg/L)	0.11	0.11	0.12	0.17	<0.01	0.13	0.07	0.10
NO_3^- (mg/L)	2.02	1.90	1.01	1.10	<0.01	1.03	2.02	2.21
PO_4^{3-} (mg/L)	0.06	0.05	0.07	0.05	0.04	0.05	0.05	0.05
SO_4^{2-} (mg/L)	5.40	5.74	8.47	8.72	5.24	5.37	5.21	5.75
HCO_3^- (mg/L)	72.0	68.3	81.8	83.0	83.0	79.3	43.9	43.9
TDS (mg/L)	106	104	122	124	117	116	68.2	142
Δ ion balance (%)	−1.00	8.06	1.45	2.43	−0.61	3.26	−3.51	3.32
Measuring point	DQ-1	DQ-1	DQ-2	DQ-2	TQ-1	TQ-1	GO-C	
Date	06/09	14/09	06/09	14/09	04/09	14/09	14/09	
T (°C)	7.1	8.3	6.7	7.4	5.7	6.1	9.4	
κ at 25°C (µS/cm)	128	125	124	141	137	152	220	
pH	7.71	7.96	7.74	7.74	8.06	8.31	8.43	
E_H (mV)	278	392	287	311	272	354	346	
O_2 content (mg/L)	10	10	10	8	9	10	10	
O_2 saturation (%)	100	99	90	87	119	85	98	
Q (L/s)	1.90	1.21	0.47	0.64	5.7	6.1	<0.1	
Na^+ (mg/L)	1.12	1.07	1.03	1.15	0.78	0.95	2.15	
NH_4^+ (mg/L)	<0.01	<0.01	<0.01	0.04	0.02	<0.01	0.03	
K^+ (mg/L)	1.21	1.21	1.22	1.27	0.81	0.78	1.56	
Mg^{2+} (mg/L)	1.59	1.71	1.90	1.92	3.19	3.43	4.19	
Ca^{2+} (mg/L)	23.3	24.3	22.0	22.4	21.7	23.6	34.6	
Sr^{2+} (mg/L)	0.21	0.18	0.07	0.20	0.08	0.11	0.11	
F^- (mg/L)	0.06	0.06	0.06	0.07	0.06	0.08	0.07	
Cl^- (mg/L)	0.39	0.68	0.81	0.62	0.75	1.15	3.95	
NO_2^- (mg/L)	<0.01	0.01	<0.01	<0.01	0.04	<0.01	0.01	

(*Continued*)

Table A1. (Continued).

	Measuring point						
	GB-U	GBQ	GBQ	BHQ	BHQ	QDS	QDS
Br^- (mg/L)	0.12	0.14	0.12	0.11	0.12	0.13	0.16
NO_3^- (mg/L)	3.02	1.92	1.87	1.84	1.46	1.34	4.08
PO_4^{3-} (mg/L)	0.08	0.06	0.08	0.05	0.09	0.05	0.08
SO_4^{2-} (mg/L)	4.17	4.26	5.14	5.12	6.75	8.93	6.59
HCO_3^- (mg/L)	73.2	78.1	75.7	67.1	73.2	73.2	115
TDS (mg/L)	108	110	114	102	109	114	172
Δ ion balance (%)	1.80	−5.57	0.68	8.01	0.91	5.34	0.32

Note: TDS = Total dissolved solids.